

CRATERS ON MARS: GLOBAL GEOMETRIC PROPERTIES FROM GRIDDED MOLA TOPOGRAPHY. J. B. Garvin¹, S. E. H. Sakimoto², and J. J. Frawley³, ¹NASA Headquarters Office of Space Science, Code SE 300 E. Street SW Washington DC 20546, jgarvin@hq.nasa.gov, ²GEST at the Geodynamics Branch, Code 921, NASA Goddard Space Flight Center, Greenbelt, MD 20771, sakimoto@geodynamics.gsfc.nasa.gov, ³Herring Bay Geophysics at NASA Goddard Space Flight Center, Greenbelt, MD 20771.

Introduction: Impact craters serve as natural probes of the target properties of planetary crusts and the tremendous diversity of morphological expressions of such features on Mars attests to their importance for deciphering the history of crustal assembly, modification, and erosion. This paper summarizes the key findings associated with a five year long survey of the three-dimensional properties of ~ 6000 martian impact craters using finely gridded MOLA topography. Previous efforts [Garvin et al. 2000, Garvin et al., 1998] have treated representative subpopulations, but this effort treats global properties from the largest survey of impact features from the perspective of their topography ever assimilated.

With the *Viking* missions of the mid-1970's, the most intensive and comprehensive robotic expeditions to any Deep Space location in the history of humanity were achieved, with scientifically stunning results associated with the morphology of impact craters. The relationships illustrated in Tables 1 and 2 suggest that

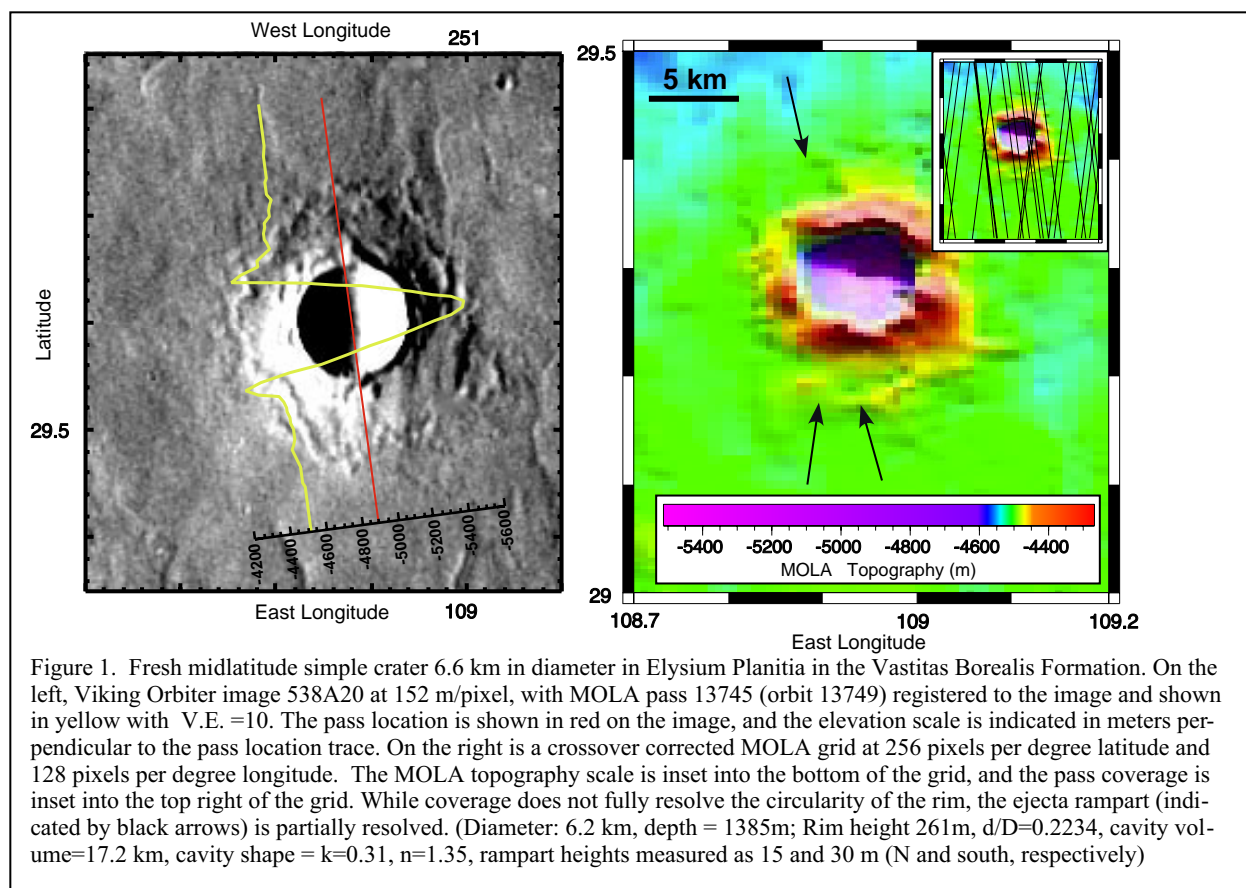
martian impact features are remarkably sensitive to target properties and to the local depositional processes.

Basic Geometric Properties: Martian craters have been studied previously from the standpoint of morphology with simple, yet rigorous treatment of crater aspect ratios, cast as crater depth d versus crater diameter D (d/D). We have previously described the rigorous set of geometric properties (i.e., Garvin et al. 2000) that we have semi-autonomously measured from MOLA topographic grids with horizontal resolution in the 0.1 to 1 km range, depending on latitude. First we treat an example to illustrate our approach.

Simple craters: Figure 1 shows an example of a fresh simple mid-latitude crater in Elysium Planitia midway between Elysium Mons and Isidis Basin within the southernmost reach of the grooved member (*Hvg*) of the Vastitas Borealis Formation. The crater is small enough and near enough the equator that the MOLA gridded data is inadequate for detailed obser-

Table 1. Diameter Dependent Impact Crater Parameters and Relationships

Parameter		Simple crater relationship	Complex crater relationship	Large crater relationship	Comments
depth	d	$d=0.21D^{0.81}$	$d=0.36D^{0.49}$		Fit to profile data for simple craters, DEM data for complex and large craters.
Rim height	H	$h=0.04D^{0.31}$	$h=0.02D^{0.84}$	$h=0.12D^{0.35}$	Complex 7-100 km, large >100km. Used DEM and Profile data.
Central Peak Height	h_{cp}	—	$h_{cp}=0.04D^{0.51}$	—	Not done for large or simple craters. Complex range 7-100 km. Used DEM and Profile data.
Central Peak Diameter	D_{cp}	—	$D_{cp}=0.25D^{1.05}$	—	Not done for large or simple craters. Complex range 7-Used DEM and Profile data. 100 km.
Cavity Shape	z	$z=0.204x^{1.76}$	$z=0.008x^{2.65}$	—	These are for profile data, for the function $z=kx^n$ as discussed in the text. Preliminary simple crater DEM data fit: $z=0.21x^{1.68}$; and complex crater DEM data fit $z=0.014x^{2.34}$
Cavity shape fit coefficient	k	$k=0.76D^{-1.17}$	$k=5.62D^{-2.51}$	—	$z=kx^n$, for profile data "good" fits
Cavity shape fit exponent	n	$n=1.04D^{0.366}$	$n=1.62x^{0.14}$	—	$z=kx^n$, for profile data "good" fits. For "good+fair" (includes central peak and polar filled craters) and "good+fair+poor" fits, the simple crater relationship does not significantly change, while the complex fit changes to $n=1.88x^{0.10}$ and $n=2.10x^{0.07}$, respectively.
Inner Cavity Wall Slope	s	$s=28.40D^{-0.18}$	$s=23.82D^{-0.28}$	—	Complex craters 7-100 km. Simple fit to profile data. Complex fit is to DEM data. Note offset of fits at transition.



variations, and the topographic parameters are primarily derived from MOLA profile data. In the Viking Orbiter image shown, the rim is clearly well-defined, and the ejecta show a modest rampart suggesting a single layer, as is also apparent in the MOLA profile data. This crater displays a cavity shape midway between parabolic and conical. In terms of cavity shape, $k=0.31$ and $n=1.35$ for this crater. At 1385 m deep for its 6.2 km diameter, the depth/diameter ratio (d/D) for this

feature is 0.2234, which is around 400 m deeper than that predicted by the global data (Table 1). This can be interpreted as either the crater being younger (and less filled) than the majority of the population used to derive the global fits, or perhaps as an indication that the target materials were conducive to enhanced excavation during crater formation. In general, we have found that the Vastitas Borealis Formation, which is included in unit 4 of our geologic unit analysis (above), has

Table 2. Geologic Unit for MOLA Gridded Data

Unit #	Simplified unit description	Simple Craters, all DEM data	Simple Craters, top 25% DEM data
1	Amazonian Surficial and Fluvial materials, Valles Marineris Floor materials, Polar Deposits, Medusae Fossae Formation, and Hesperian Fluvial Materials	$d = 0.001 D^{3.97}$ (44)	$d = 0.17 D^{0.79}$ (8)
2	Amazonian Volcanic Plains	$d = 0.156 D^{0.74}$ (46)	$d = 0.23 D^{0.74}$ (8)
3	Amazonian Volcanic Assemblages	$d = 0.165 D^{0.73}$ (88)	$d = 0.35 D^{0.46}$ (16)
4	Hesperian Northern Plains and Dorsa Argentea Formation	$d = 0.282 D^{-0.11}$ (85)	$d = 0.01 D^{2.62}$ (13)
5	Hesperian Volcanic Assemblages	$d = 0.074 D^{1.08}$ (110)	$d = 0.21 D^{0.68}$ (17)
6	Hesperian Plateau Sequence, Highly Deformed Materials, Amazonian and Hesperian Hellas Assemblage	$d = 0.189 D^{0.58}$ (122)	$d = 0.18 D^{0.78}$ (21)
7	Noachian Plateau Sequence	$d = 0.168 D^{0.56}$ (170)	$d = 0.21 D^{0.69}$ (28)
8	Noachian Highly Deformed Materials	$d = 0.367 D^{0.1}$ (81)	$d = 0.23 D^{0.61}$ (16)
9	Craters	$d = 0.18 D^{0.51}$ (104)	$d = 0.24 D^{0.63}$ (18)
Global weighted	Fits to global DEM data for simple and complex craters weighted by measured number of craters per unit.	$d = 0.18 D^{0.71}$ (850)	$d = 0.21 D^{0.84}$ (145)
Global	Fits to global profile (simple craters) and DEM (complex and large craters) data.	$d = 0.21 D^{0.8}$ (2263)	$d = 0.21 D^{0.81}$ (469)

Units and Descriptions summarized from *Scott and Tanaka*, [1986], *Greeley and Guest*, [1987], and *Tanaka and Scott*, [1987]. ([4-6] The number in parens following each fit indicates the approximate number of craters the fit is based upon.

slightly *shallower* craters than the global average for craters less than about 50 km in diameter (see Table 2), so in this case target property effects could perhaps be explained by weak, easily excavated materials. Indeed, as Table 2 suggests, surficial units likely to represent less well consolidated materials are relatively less deep at higher energies (i.e., crater diameters) than their competent unit counterparts. Simple Amazonian craters such as that illustrated in Figure 2 (i.e., within Amazonis Planitia), are reminiscent of lunar craters such as Linne, and display conical cavity geometries with steep inner cavity walls slopes (i.e., up to 16-20 degrees). Such craters are relatively rare on Mars in the broad survey of simple craters we have conducted with MOLA topographic data (profiles and grids where possible). We have begun interpolating MOC 2-5 m imaging data atop 100-500m scale MOLA topographic grids to provide more quantitative insights into the behavior of fresh simple craters on Mars, especially across "softer" units such as #4 above.

Conclusions: The wealth of new Martian topographic data allow study of martian craters at a level of detail and rigor unprecedented in planetary sciences. The global database of thousands of topographically characterized craters generated is revealing aspects of crater topography and target properties that may affect areas of Mars research from surface ages and properties to the mechanics of cratering. This progress report only highlights a few of the observations and correlations we have developed for our dataset.

References:

[1] Garvin, J. B. and J. J. Frawley (1998). Geophysical Research Letters 25(24): 4405-4408. [2] Garvin, J. B., S. E. H. Sakimoto, et al. (1998). Lunar and Planetary Science XXIX, Houston, TX, Lunar and Planetary Institute, Houston (CD-ROM). Garvin, J. B., S. E. H. Sakimoto, et al. (2000). LPSC XXI, Houston, TX CDROM: Abstract # 1619. [3] Garvin, J. B., S. E. H. Sakimoto, et al. (2000). "North Polar Region Craterforms on Mars: Geometric Characteristics from the Mars Orbiter Laser Altimeter." Icarus 144(April): 329-352. [4] Garvin, J. B., S. E. H. Sakimoto, et al. (1999). The Fifth International Conference on Mars, Pasadena, CA, Lunar and Planetary Institute, Houston (CD-ROM). [4] Greeley, R. and J. E. Guest (1987). Geologic Map of the eastern equatorial region of Mars, U.S. Geol. Surv. Misc. Invest. [5] Scott, D. H. and K. L. Tanaka (1986). Geologic Map of the western equatorial region of Mars, U.S. Geol. Surv. Misc. Invest. [6] Tanaka, K. L. and D. H. Scott (1987). Geologic map of the polar regions of Mars, USGS.

Figure 2. a simple crater with MOLA topography and MOC image coverage.

